

Supporting Information For:

**Record High Single-Ion Magnetic Moments through $4f^n5d^1$
Electron Configurations in the Divalent Lanthanide Complexes
 $[(C_5H_4SiMe_3)_3Ln]^-$**

Katie R. Meihaus,[†] Megan E. Fieser,[‡] Jordan F. Corbey,[‡] William J. Evans,^{‡,*} and Jeffrey R.
Long^{†,§,*}

[†]*Department of Chemistry, University of California, Berkeley, California 94720*

[‡]*Department of Chemistry, University of California, Irvine, California 92697*

[§]*Materials Science Division, Lawrence Berkeley National Laboratory, Berkeley, California
94720*

Journal of the American Chemical Society

Table of Contents

Page S3 – Figure S1, Plot of the magnetic susceptibility times temperature ($\chi_M T$) versus T for the stable trivalent lanthanides, cerium through ytterbium.

Page S4 – Figure S2, Plot of $\chi_M T$ versus T for $\text{Cp}'_3\text{Sm}$ / $[\text{K}(\text{crypt-222})][\text{Cp}'_3\text{Sm}]$ and $\text{Cp}'_3\text{Tm}$ / $[\text{K}(\text{crypt-222})][\text{Cp}'_3\text{Tm}]$.

Page S5 – Figure S3, Magnetization versus field curves for $[\text{K}(2.2.2\text{-cryptand})][\text{Cp}'_3\text{Gd}]$.

Page S6 – Figure S4, Plot of $\chi_M T$ versus T for $[\text{K}(\text{crypt-222})][\text{Cp}'_3\text{Y}]$ and $[\text{K}(\text{crypt-222})][\text{Cp}'_3\text{La}]$.

Page S7 – Figure S5, Plot of $\chi_M T$ versus T for $[\text{K}(2.2.2\text{-cryptand})][\text{Cp}'_3\text{Tb}]$ / $\text{Cp}'_3\text{Tb}$ and $\text{Cp}'_3\text{Er}$ / $[\text{K}(2.2.2\text{-cryptand})][\text{Cp}'_3\text{Er}]$

Page S8 – Figure S6, Plot of $\chi_M T$ versus T for $\text{Cp}'_3\text{Ce}$ / $[\text{K}(\text{crypt-222})][\text{Cp}'_3\text{Ce}]$ and $\text{Cp}'_3\text{Pr}$ / $[\text{K}(\text{crypt-222})][\text{Cp}'_3\text{Pr}]$.

Page S9 – Figure S7, Variable-field $\chi_M T$ versus T for $[\text{K}(\text{crypt-222})][\text{Cp}'_3\text{Ce}]$ and $[\text{K}(\text{crypt-222})][\text{Cp}'_3\text{Nd}]$.

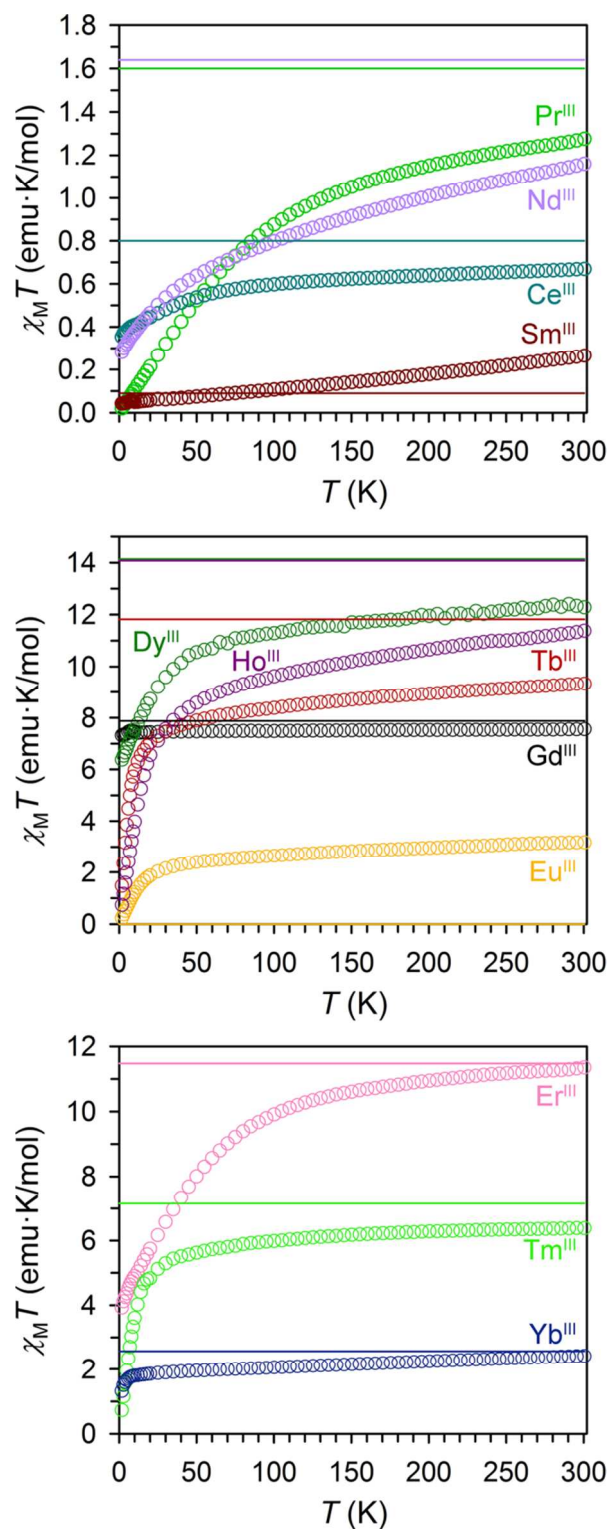


Figure S1. Plot of the magnetic susceptibility times temperature ($\chi_M T$) versus temperature for the stable trivalent lanthanides, cerium through ytterbium. Colored circles correspond to experimental data and colored lines represent the theoretical room temperature $\chi_M T$ value for each of the free trivalent lanthanides.

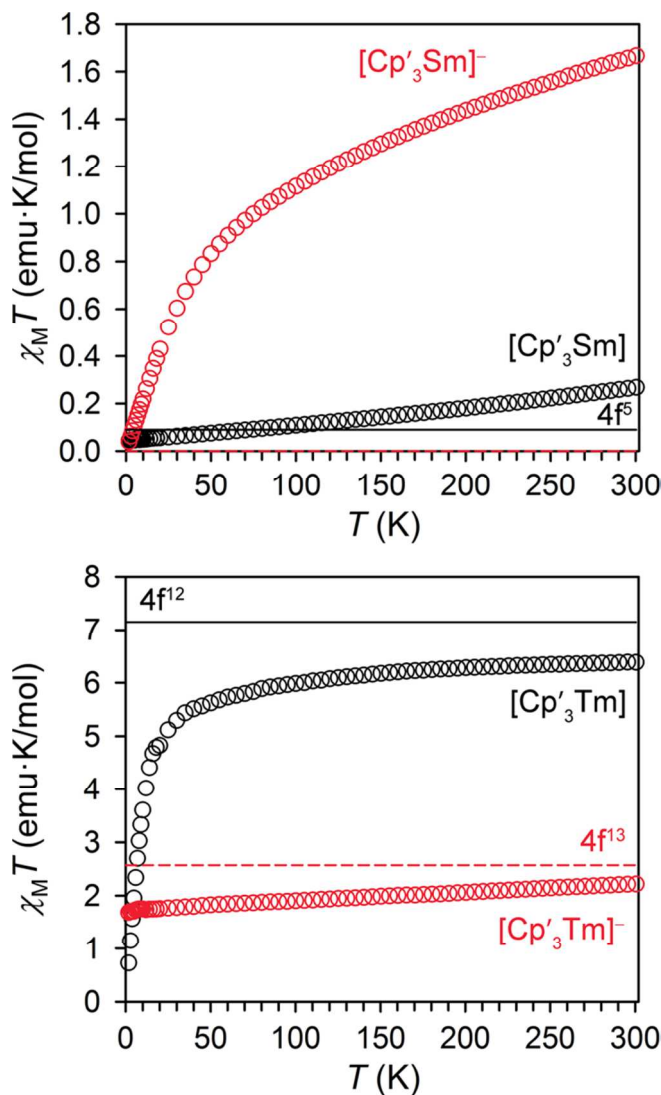


Figure S2. (Top) Plot of the magnetic susceptibility times temperature ($\chi_M T$) versus temperature for $\text{Cp}'_3\text{Sm}$ (black circles) and $[\text{K}(\text{crypt-222})][\text{Cp}'_3\text{Sm}]$ (red circles) under an applied field of 0.1 T. Solid black and dashed pink lines represent the theoretical room temperature values for free Sm^{III} ($4f^5$) and Sm^{II} ($4f^7$), respectively. For $[\text{K}(\text{crypt-222})][\text{Cp}'_3\text{Sm}]$ at $T = 300$ K, $\chi_M T$ is 1.66 $\text{emu} \cdot \text{K/mol}$, larger than the theoretical value of 0 $\text{emu} \cdot \text{K/mol}$, assuming only the ground state ($S = 3$, $L = 3$, $J = 0$) is populated. However, the energy separation between ground and excited J for Sm^{II} and isoelectronic Eu^{III} is $\sim 300 \text{ cm}^{-1}$, thus due to population of excited J states, the room temperature moment is often larger than the theoretical prediction. (Bottom) Plot of the magnetic susceptibility times temperature ($\chi_M T$) versus temperature for $\text{Cp}'_3\text{Tm}$ (black circles) and $[\text{K}(\text{crypt-222})][\text{Cp}'_3\text{Tm}]$ (red circles) under an applied field of 0.1 T. Solid black and dashed pink lines represent the theoretical room temperature values for free Tm^{III} ($4f^{12}$) and Tm^{II} ($4f^{13}$), respectively. The experimental room temperature $\chi_M T$ values of 6.38 $\text{emu} \cdot \text{K/mol}$ and 2.22 $\text{emu} \cdot \text{K/mol}$ both closely approach the predicted values for free Tm^{III} (7.15 $\text{emu} \cdot \text{K/mol}$) and Tm^{II} (2.57 $\text{emu} \cdot \text{K/mol}$).

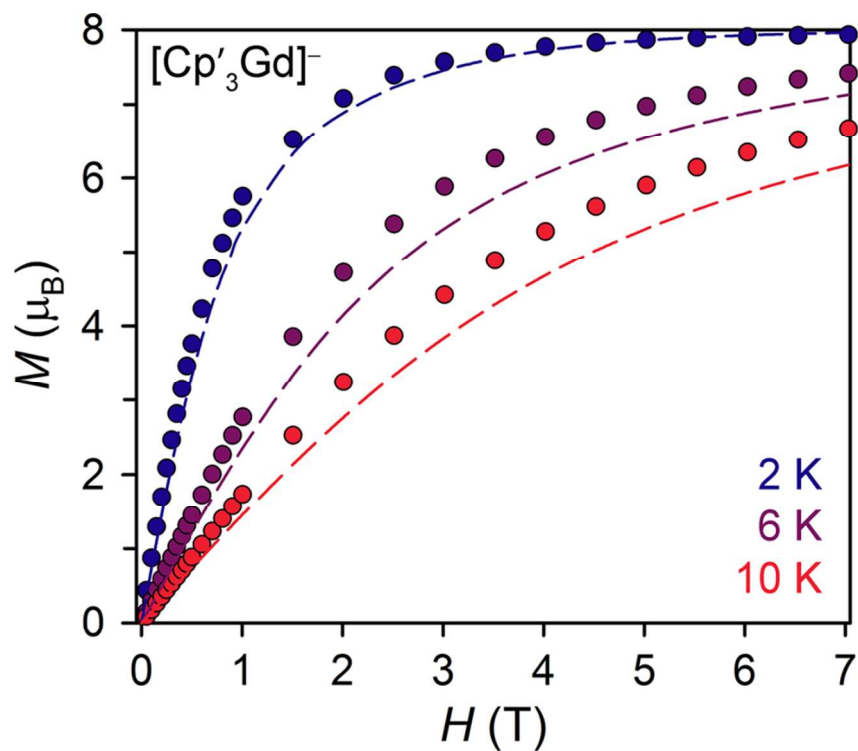


Figure S3. Variable temperature $M(H)$ curves for $[\text{K}(2.2.2\text{-cryptand})][\text{Cp}'_3\text{Gd}]$ collected from zero to 7 T. Data points are given by colored spheres and dashed lines represent the corresponding sum of an $S = \frac{1}{2}$ and $S = \frac{7}{2}$ Brillouin function.

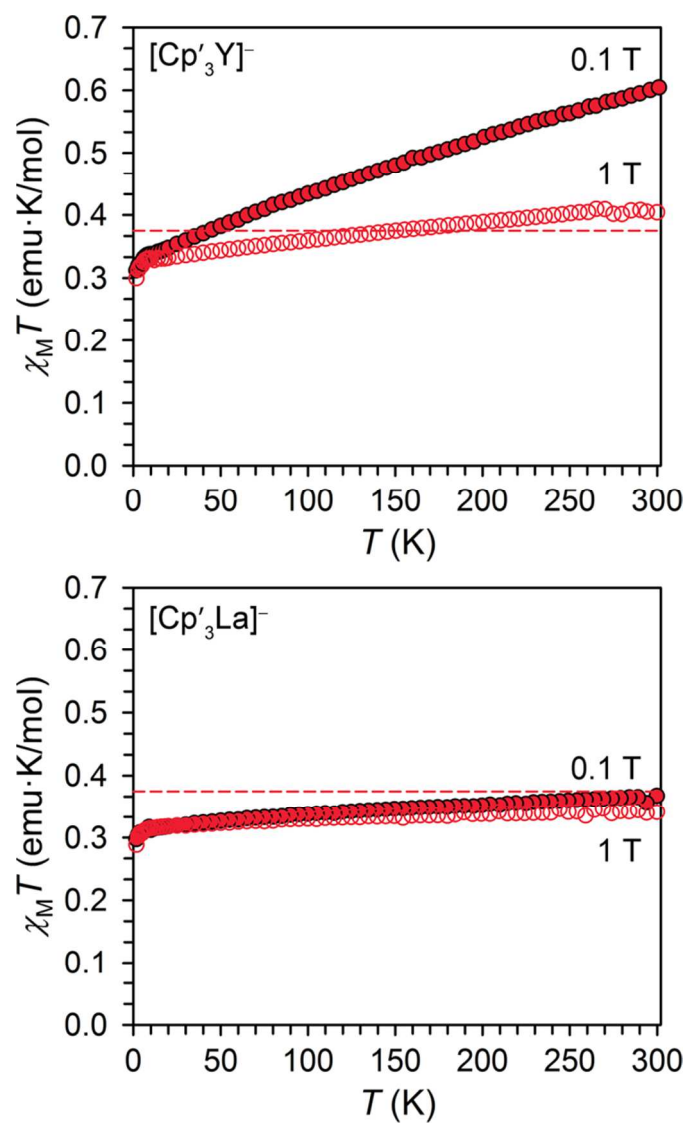


Figure S4. Plot of the magnetic susceptibility times temperature ($\chi_M T$) versus temperature for [K(crypt-222)][Cp'₃Y] (top) and [K(crypt-222)][Cp'₃La] (bottom) under applied fields of 0.1 T (filled circles) and 1 T (empty circles). Solid dashed pink lines represent the theoretical room temperature $\chi_M T$ values = 0.375 emu·K/mol for $S = 1/2$. The large slope and linear increase with temperature in the case of [K(crypt-222)][Cp'₃Y] is indicative of temperature independent paramagnetism.

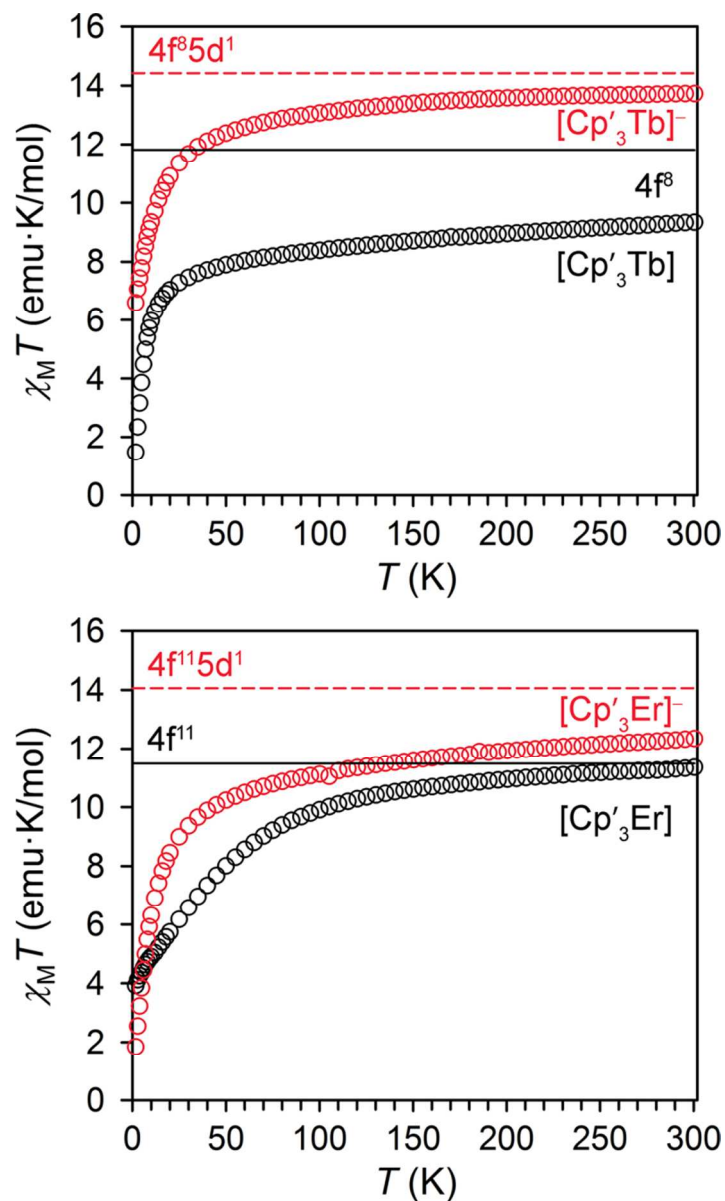


Figure S5. (Top) Plot of the static magnetic susceptibility times temperature ($\chi_M T$) versus T collected at 0.1 T for $\text{Cp}'_3\text{Tb}$ (black circles) and $[K(2.2.2\text{-cryptand})][\text{Cp}'_3\text{Tb}]$ (red circles), with room temperature $\chi_M T$ values of 13.73 emu·K/mol and 9.34 emu·K/mol, respectively. Dashed pink line and solid black line represent the theoretical $\chi_M T$ values at 300 K for free Tb^{II} (14.42 emu·K/mol, coupled $4f^8 5d^1$) and free Tb^{III} (11.82 emu·K/mol). (Bottom) Plot of the static magnetic susceptibility times temperature ($\chi_M T$) versus T collected at 0.1 T for $\text{Cp}'_3\text{Er}$ (black circles) and $[K(2.2.2\text{-cryptand})][\text{Cp}'_3\text{Er}]$ (red circles), with room temperature $\chi_M T$ values of 12.35 emu·K/mol and 11.35 emu·K/mol, respectively. Dashed pink line and solid black line represent the theoretical $\chi_M T$ values at 300 K for free Er^{II} (14.06 emu·K/mol, coupled $4f^{11} 5d^1$) and free Er^{III} (11.48 emu·K/mol).

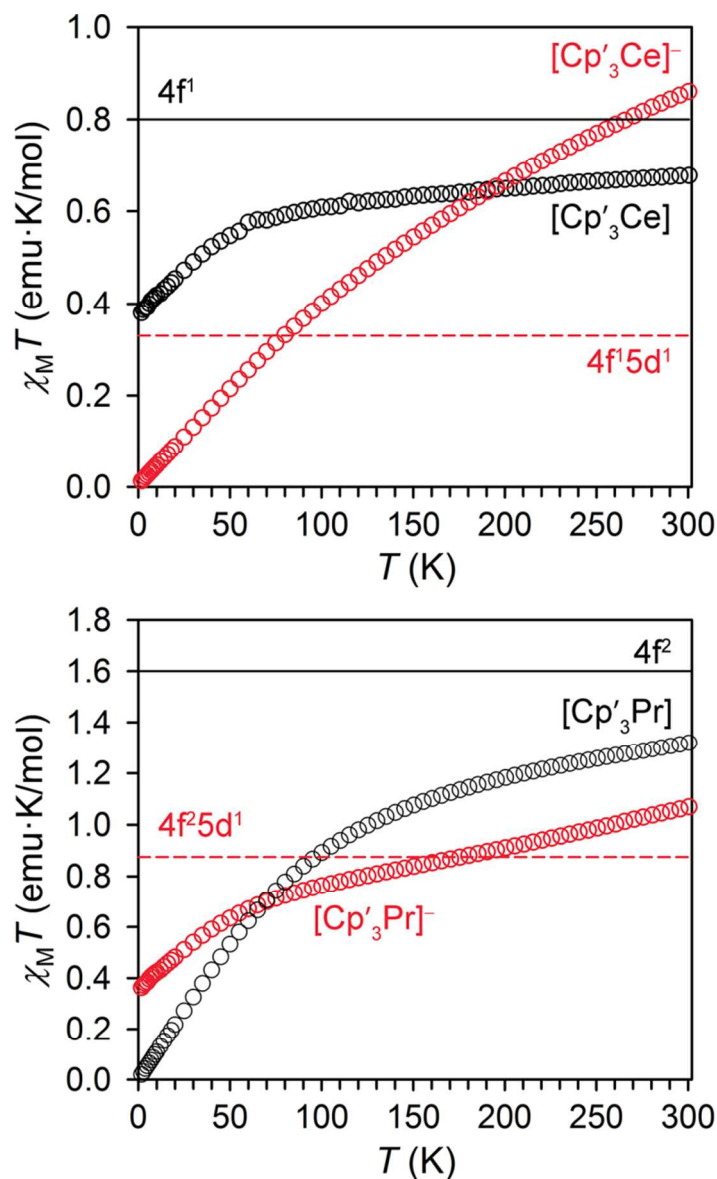


Figure S6. (Top) Plot of the magnetic susceptibility times temperature ($\chi_M T$) versus temperature for $\text{Cp}'_3\text{Ce}$ (black circles) and $[\text{K}(\text{crypt-222})][\text{Cp}'_3\text{Ce}]$ (red circles) under an applied field of 0.1 T. Solid black and dashed pink lines represent the theoretical room temperature values for free Ce^{III} ($4f^1$) and Ce^{II} (assuming $4f^1 5d^1$), respectively. For $[\text{K}(\text{crypt-222})][\text{Cp}'_3\text{Ce}]$ at $T = 300$ K, $\chi_M T$ is 0.86 emu·K/mol, larger than the theoretical value for the coupled $4f^1 5d^1$ configuration (0.33 emu·K/mol), though smaller than the theoretical value for the $4f^2$ and uncoupled $4f^1 5d^1$ configurations (1.6 emu·K/mol and 1.18 emu·K/mol, respectively). (Bottom) Plot of the magnetic susceptibility times temperature ($\chi_M T$) versus temperature for $\text{Cp}'_3\text{Pr}$ (black circles) and $[\text{K}(\text{crypt-222})][\text{Cp}'_3\text{Pr}]$ (red circles) under an applied field of 0.1 T. Solid black and dashed pink lines represent the theoretical room temperature values for free Pr^{III} ($4f^2$) and Pr^{II} ($4f^2 5d^1$ coupled), respectively. The room temperature $\chi_M T$ value of 1.07 emu·K/mol for $[\text{K}(\text{crypt-222})][\text{Cp}'_3\text{Pr}]$ falls in between the values for the $4f^2$ and $4f^2 5d^1$ configurations, similar to Ce^{II} and Nd^{II} as discussed in the main text.

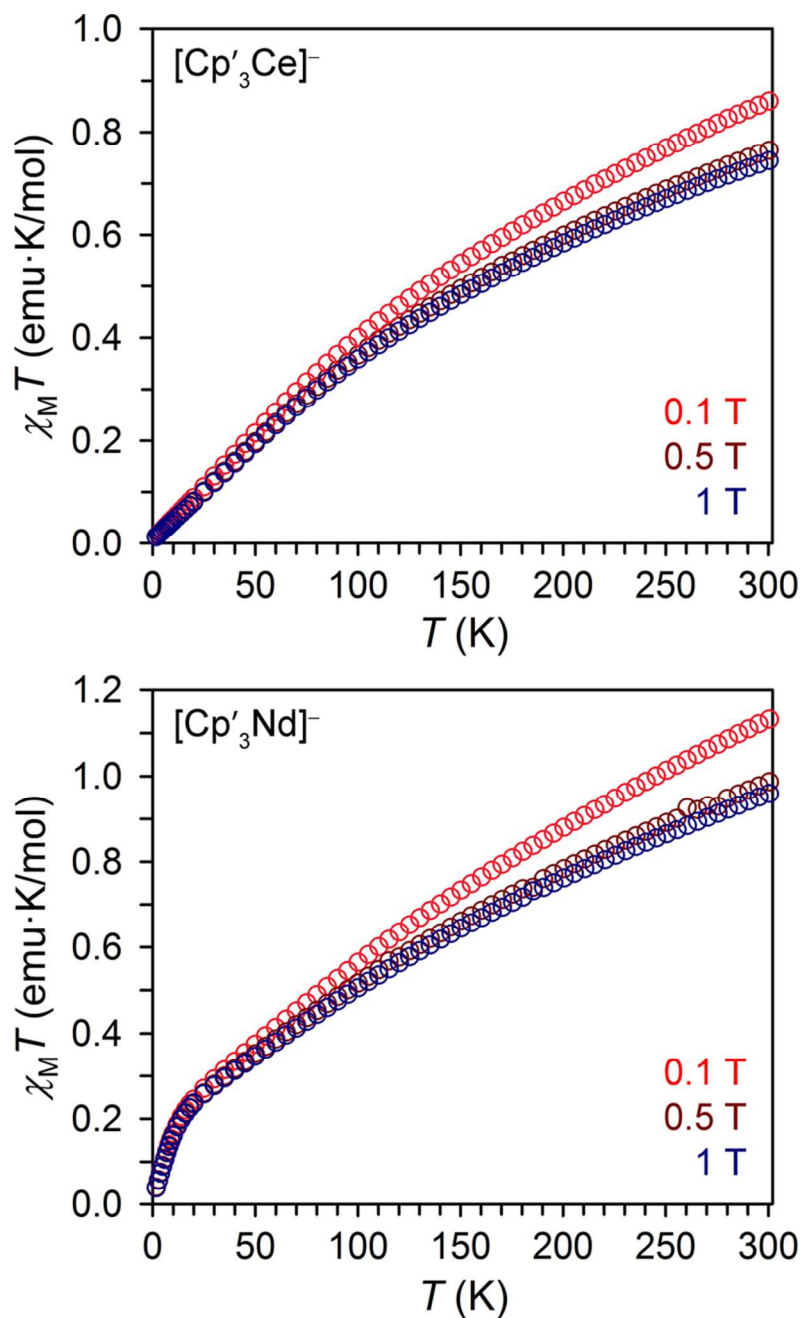


Figure S7. Plot of the magnetic susceptibility times temperature ($\chi_M T$) versus temperature for $[\text{K}(\text{crypt-222})][\text{Cp}'_3\text{Ce}]$ (top) and $[\text{K}(\text{crypt-222})][\text{Cp}'_3\text{Nd}]$ (bottom) collected at fields of 0.1 T, 0.5 T, and 1 T (red, dark red, and dark blue circles, respectively).